Urinary single-cell sequencing captures kidney injury and repair processes in human acute kidney injury

see commentary on page 1219

OPEN

Jan Klocke[1,2], Seung Joon Kim[3], Christopher M. Skopnik[1,2], Christian Hinze[1,4,5], Anastasiya Boltengagen[3], Diana Metzke[1,2], Emil Grothgar[1,2], Luka Prskalo[1,2], Leonie Wagner[1,2], Paul Freund[1,2], Nina Görlich[1,2], Frédéric Muench[1], Kai M. Schmidt-Ott[1,4,5], Mir-Farzin Mashreghi[6], Christine Kocks[3], Kai-Uwe Eckardt[1,7], Nikolaus Rajewsky[3,7] and Philipp Enghard[1,2,7]

[1]Department of Nephrology and Medical Intensive Care, Charité-Universitätsmedizin, Berlin, Corporate Member of Freie Universität Berlin and Humboldt-Universität zu Berlin, Berlin, Germany; [2]Deutsches Rheuma-Forschungszentrum, an Institute of the Leibniz Foundation, Berlin, Germany; [3]Systems Biology of Gene-Regulatory Elements, Berlin Institute for Medical Systems Biology (BIMSB), Max-Delbrück-Center for Molecular Medicine in the Helmholtz Association (MDC), Berlin, Germany; [4]Molecular and Translational Kidney Research, Max-Delbrück-Center for Molecular Medicine in the Helmholtz Association (MDC), Berlin, Germany; [5]Department of Nephrology and Hypertension, Hannover Medical School, Hannover, Germany; and [6]Therapeutic Gene Regulation, Deutsches Rheuma-Forschungszentrum, an Institute of the Leibniz Foundation, Berlin, Germany

Acute kidney injury (AKI) is a major health issue, the outcome of which depends primarily on damage and reparative processes of tubular epithelial cells. Mechanisms underlying AKI remain incompletely understood, specific therapies are lacking and monitoring the course of AKI in clinical routine is confined to measuring urine output and plasma levels of filtration markers. Here we demonstrate feasibility and potential of a novel approach to assess the cellular and molecular dynamics of AKI by establishing a robust urine-to-single cell RNA sequencing (scRNAseq) pipeline for excreted kidney cells via flow cytometry sorting. We analyzed 42,608 single cell transcriptomes of 40 urine samples from 32 patients with AKI and compared our data with reference material from human AKI post-mortem biopsies and published mouse data. We demonstrate that tubular epithelial cells transcriptomes mirror kidney pathology and reflect distinct injury and repair processes, including oxidative stress, inflammation, and tissue rearrangement. We also describe an AKI-specific abundant urinary excretion of adaptive progenitor-like cells. Thus, single cell transcriptomics of kidney cells excreted in urine provides noninvasive, unprecedented insight into cellular processes underlying AKI, thereby opening novel opportunities for target identification, AKI sub-categorization, and monitoring of natural disease course and interventions.

Kidney International (2022) **102,** 1359–1370; https://doi.org/10.1016/j.kint.2022.07.032

KEYWORDS: acute kidney injury; distal tubule; gene expression

Correspondence: *Jan Klocke, Department of Nephrology and Medical Intensive Care, Charité-Universitätsmedizin Berlin, Charitéplatz 1, 10117 Berlin, Germany. E-mail: jan.klocke@charite.de*

[7]K-UE, NR, and PE jointly supervised the work and contributed equally.

Received 3 March 2022; revised 6 July 2022; accepted 27 July 2022; published online 29 August 2022

Acute kidney injury (AKI) is a major health concern associated with significant morbidity and mortality.[1,2] Causal therapies for preventing AKI or improving its recovery are still missing. Kidney tubular epithelial cells (TECs) are the primarily affected cells in AKI and a key component in the resulting inflammation and healing processes.[3–6]

Research on AKI and on the role of TECs must overcome 3 major challenges: (i) finding a suitable way to study human disease pathomechanisms or effectively translate findings from mouse models to the human setting, (ii) providing clinicians with meaningful biomarkers to predict outcomes, and (iii) understanding TEC repair to enable strategies to enhance regeneration and reduce scarring.[7] It is reasonable to believe that answers to all 3 challenges may lie in the urine.

Transcriptomic analyses in mouse AKI models on the single-cell level have rapidly enhanced and transformed our understanding of injured and recovering TEC states.[5,6,8–10] Recently, the first biopsy-based human single-cell studies of the kidney and AKI have been reported.[8,11,12] However, the invasive nature of kidney biopsies limits scalability and represents a hurdle for translation into clinical routine. In contrast, analysis of kidney cells excreted in urine may provide noninvasive insights into altered cell physiology in both inflammation[13–16] and injury.[17] The feasibility of urinary single-cell RNA sequencing (scRNA-seq) has been proven in chronic kidney diseases, such as diabetic nephropathy and focal segmental glomerular sclerosis,[18–20] and indicates that the urine has untapped potential as a source for the noninvasive study of kidney epithelial cells. Moreover, urine-derived progenitor or stem cells, which were first isolated in pediatric patients,[21] have since been studied extensively.[22] They are now a common source for inducible pluripotent stem cells[23] and can be detected even in healthy individuals.[20]

Therefore, we hypothesized that urinary TECs, which are excreted with the urine after kidney damage, may be an apt target to study inflammation and regeneration in AKI via urinary scRNAseq. By analyzing 40 urine samples from 32 individuals with AKI, we observed different injury-related cell states that mirror findings from mouse disease models and human AKI kidney tissue.

METHODS

Patients

We collected 40 urine samples of 32 patients with AKI, as defined by Kidney Disease: Improving Global Outcomes (KDIGO) criteria (Supplementary Figure S1 and Supplementary Table S1). Patients were sampled at a variable time point within the first 21 days after AKI onset. Seven patients underwent cardiac surgery within a maximum of 48 hours before AKI onset, and 15 patients were admitted to intensive care units because of pneumonia (all fulfilling sepsis criteria) and developed AKI during the first 5 days of their intensive care unit stay; most of these patients (14/15) had coronavirus disease 2019 (COVID-19). An additional 10 patients had other, mostly prerenal, causes of AKI, including gastrointestinal bleeding (n = 1), diarrhea (n = 2), exsiccosis (n = 4), or decompensated heart failure (n = 3). For detailed patient characteristics, see also Supplementary Methods.

Sample preparation and single-cell sequencing

Samples were collected as first morning void urine or via urinary catheter (using the pooled urine output of 4 hours). Viable cells were sorted using a flow cytometric approach (Supplementary Figure S2). Some samples were barcoded, pooled, and later demultiplexed (Supplementary Figure S3). Single cells were sequenced following the 10x Genomics protocol for Chromium Next GEM Single Cell 3' v3.1 chemistry (10x Genomics). For details, see the Supplementary Methods.

Statistical analysis

All RNA-sequencing data were analyzed using R.[24] Normalization, logarithmic transformation, identification of highly variable features, scaling, principal component analysis, and extraction of differentially expressed features were done using Seurat. For detailed description, see Supplementary Methods. Significant differences between cell counts were tested using 2-tailed unpaired 2-sample Wilcoxon test.

Study approval

The ethics committee of Charité University Hospital approved the study (Charité EA2/141/19). Informed consent was obtained from all patients or next of kin before participation.

RESULTS

Urine cellular composition is representative for major kidney and immune cell types

The first goal of our study was to understand what cell types occur in the urine sediment after AKI. Therefore, we performed scRNAseq on sediment derived from 40 fresh urine samples of 32 patients (Supplementary Table S1 and Supplementary Figure S1). We collected samples at different time points 0 to 21 days after onset of AKI due to cardiac surgery (n = 7), pneumonia (n = 15; among them 14 cases of COVID-19), or prerenal causes (n = 10). After quality control filtering, we obtained a total of 42,608 single cells with a median of 472 cells per sample as well as 1436 detected genes and 3991 unique transcripts per cell.

Data analysis (uniform manifold approximation and projection visualization, unbiased clustering, and annotation based on known marker genes) revealed 3 cell type categories to be the main features of the AKI urine sediment (Figure 1 and Supplementary Table S2): *Renal parenchymal cells* were composed of a small, homogeneous fraction of podocytes ("PDCs"; *NPHS2* and *PODXL*) and many cells from the renal tubules ("TECs"; *CRYAB* and *EPCAM*) with various injury reactive traits, which are detailed further below. *Immune cells* included a dominant myeloid signal with multiple monocyte/macrophage subsets showing tissue residency[25] ("MO_kdnrs"; *C1QB* and *CD74*), proinflammatory ("MO_infl"; *IL1B* and *TIMP1*), profibrotic[26,27] ("MO_SPP1+"; *SPP1* and *ALOX5AP*), antioxidative ("MO_MT+"; various metallothionein genes), or severely injured ("MO_dmg") phenotypes. Granulocytes were excluded from the analysis via flow sort (Supplementary Figure S2) and are featured herein only as a small residual cluster ("GRAN"; *CSF3R* and *MNDA*). Lymphocytes were also regularly featured, with T cells being more frequent than B cells. Finally, cells from the *urogenital tract* ("UGECs") included epithelia from the reproductive system (*KRT13* and *PSCA*) and urothelial cells expressing uroplakins (*UPK2*).

Interestingly, all 3 of these major cell types were detectable across most AKI samples (Supplementary Figures S4 and S5), despite a diverse overall quantity of captured high-quality single-cell transcriptomes, with a median of 472 (range, 8–5900) cells/sample (Supplementary Figure S4D). UGECs were featured more prominently in female patients (Figure 1b and d and Supplementary Figure S5).

Thus, we asked whether other factors also influence the cellular urine composition in AKI. Therefore, we examined the different AKI entities separately and compared our data with public urine cell data sets. Briefly, healthy control urine (GSE157640)[18] consisted almost entirely of UGECs, whereas all examined AKI entities and chronic diseases, like diabetic nephropathy and focal segmental glomerular sclerosis, included leukocytes and kidney parenchymal cells to varying degrees. Severe acute respiratory syndrome coronavirus 2 (SARS-CoV-2) infection also altered the AKI urine signature in our own data (for more detailed information on these cross-disease comparisons, see Supplementary Results and Supplementary Figures S15–S20). Overall, urine samples from patients with AKI regularly featured immune and most importantly epithelial cells from the kidney, potentially reflecting type and severity of kidney damage.

Urinary kidney epithelial cells display different injured and adaptive cell states

To use urinary cellular analysis as a proxy for AKI pathophysiology, it is crucial to know which kidney features are released into the urine and how detailed those cells can be

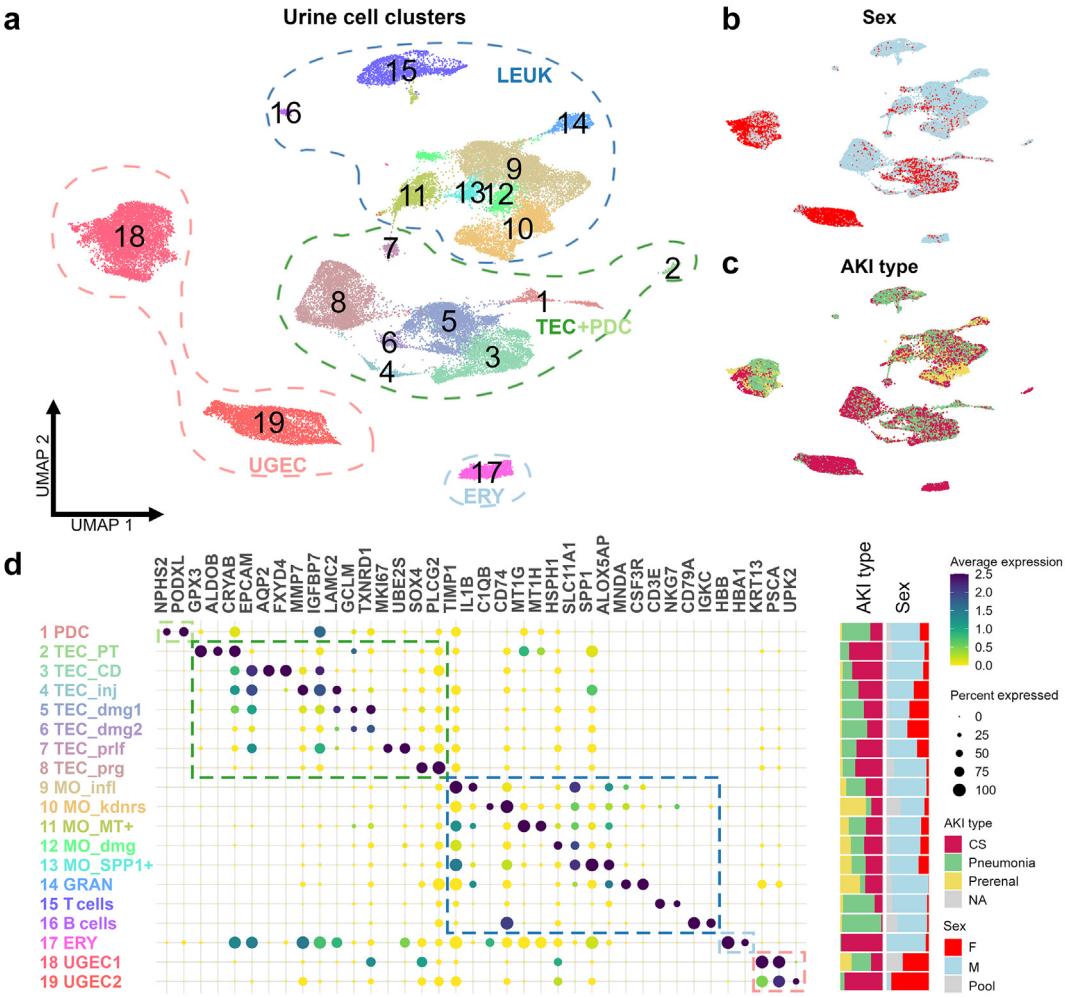

Figure 1 | Cellular composition of urine in acute kidney injury (AKI) is diverse and individual, but representative for major epithelial and immune cell types. (**a**) Uniform manifold approximation and projection (UMAP) of 42,608 single-cell RNA-sequencing urine cells from 32 individuals with AKI. Cellular composition is individually diverse but can be broadly grouped into kidney cells (podocytes [PDCs] and tubular epithelial cells [TECs]), urogenital epithelial cells (UGECs), and leukocytes (LEUKs) with sporadic contamination of erythrocytes (ERYs). See Supplementary Figure S4 for detailed sample information. (**b,c**) Distribution of cells in UMAP by sex (**b**) and etiology of AKI (**c**). Female (F) patients (red) excrete more UGECs via urine (see also Supplementary Figure S5). Patients with (mild) prerenal causes of AKI (yellow) excrete mainly myeloid cells and UGECs and fewer TECs than cardiac surgery (CS)–associated AKI (red) or pneumonia (green); also note Supplementary Results. (**d**) Dot plot of marker gene expression for each cell type. CD, collecting duct; dmg, damaged; GRAN, granulocyte; infl, inflammatory; inj, injured; kdnrs, kidney resident; M, male; MO, monocyte/macrophage; MT, metallothioneins; prg, progenitor-like; prlf, proliferating; PT, proximal tubule; *SPP1*, osteopontin.

characterized. For that reason, we reanalyzed the 12,853 AKI single-cell transcriptomes that were identified as TECs or PDCs before (Figure 2a, Supplementary Figure S6, and Supplementary Table S3): In this focused analysis on renal parenchymal cells, 10 cell subsets resembled cells from different segments of the renal tubule system with expression of specific marker genes (Figure 2b and Supplementary Figure S7). However, several key segment markers were not regularly expressed in these clusters (e.g., *MME* or *LRP2* in proximal tubule [PT] cells), hinting at a beginning dedifferentiation process. Those "canonical" clusters (summarized as "TEC_cnn") only composed a small fraction of urinary TECs, whereas most other transcriptomes showed one of several injury-related cell states (Figure 2c–f): A large group of cells ("TEC_inj"; Figure 2c) combined high expression of injury markers (*LCN2*, *IGFBP7*, and *KRT8*) with proinflammatory cytokines and chemokines (*IL32*, *CD40*, *CCL2*, and *IFIT1-3*) and *epithelial-to-mesenchymal transition* markers (*VIM* and *MMP7*). *Oxidative stress* signatures (*TXNRD1*, *GCLM*, and *SLC7A11*) were dominant in another group ("TEC_str"; Figure 2d).

Particularly interesting were potentially regenerating cells showing *proliferation* (*CENPF* and *MKI67*; "TEC_prlf"; Figure 2f) and a large subset expressing transcription factors connected to kidney development and repair (*SOX4*, *SOX9*, and *PAX2*), presumably reflecting a dedifferentiated adaptive

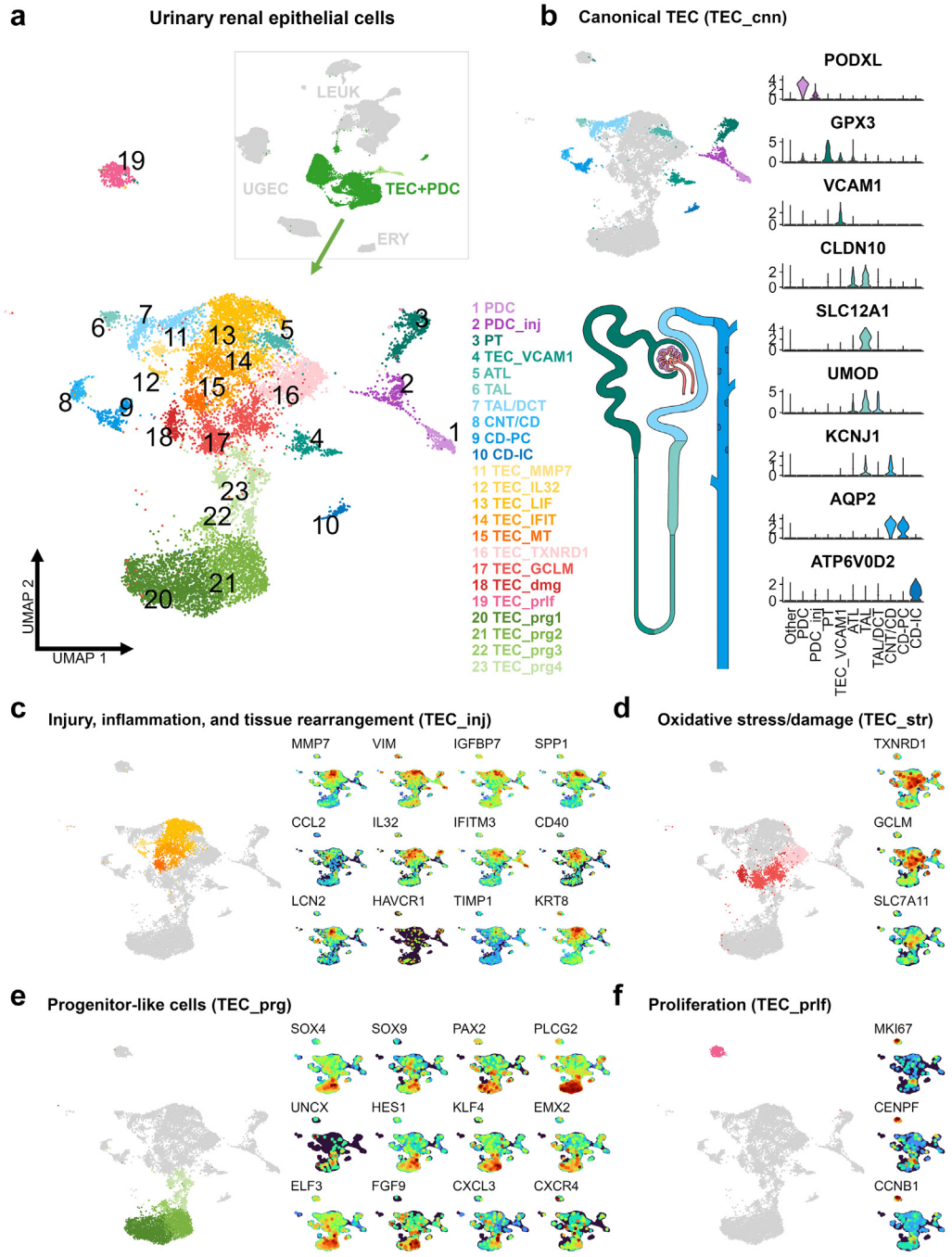

Figure 2 | Urinary kidney epithelial cells display different injured and adaptive cell states. (**a**) Uniform manifold approximation and projection (UMAP) of 12,853 urinary renal parenchymal single-cell RNA-sequencing transcriptomes from 32 individuals with acute kidney injury in 23 distinct clusters. See Supplementary Figure S6 for detailed description of clusters. Clusters can be grouped into 5 major groups. (**b**) Canonical renal cells (TEC_cnn), including tubular cells from the proximal tubule (PT), thin limb (TEC_VCAM1/ATL), thick ascending limb (TAL), distal convoluted tubule (DCT), connecting tubule (CNT), collecting duct principal cells (CD-PCs), collecting duct intercalated cells (CD-ICs), as well as podocytes (PDCs); see violin plot and Supplementary Figure S7 for detailed marker genes. (**c**–**f**) Tubular epithelial cell (TEC) clusters with markers for injury, inflammatory and epithelial-to-mesenchymal transition (**c**), oxidative stress (**d**), progenitor/dedifferentiation markers (**e**), and proliferation markers (**f**). ATL, ascending thin limb; ATP6V0D2, ATPase H+ Transporting V0 Subunit D2; CLDN10, claudin 10; dmg, damaged; ERY, erythrocyte; GCLM, glutamate-cysteine ligase modifier subunit; GPX3, glutathione peroxidase 3; IFIT, interferon induced protein with tetratricopeptide repeats; inj, injured; KCNJ1, potassium inwardly rectifying channel subfamily J member 1; IL32, interleukin 32; LIF, leukemia inhibitory factor; MMP7, matrix metalloproteinase 7; MT, metallothioneins; PODXL, podocalyxin-like protein 1; prg, progenitor-like; prlf, proliferating; SLC12A1, solute carrier family 12 member 1; TXNRD1, thioredoxin reductase 1; UGEC, urogenital epithelial cell; UMOD, uromodulin; VCAM1, vascular cell adhesion protein 1.

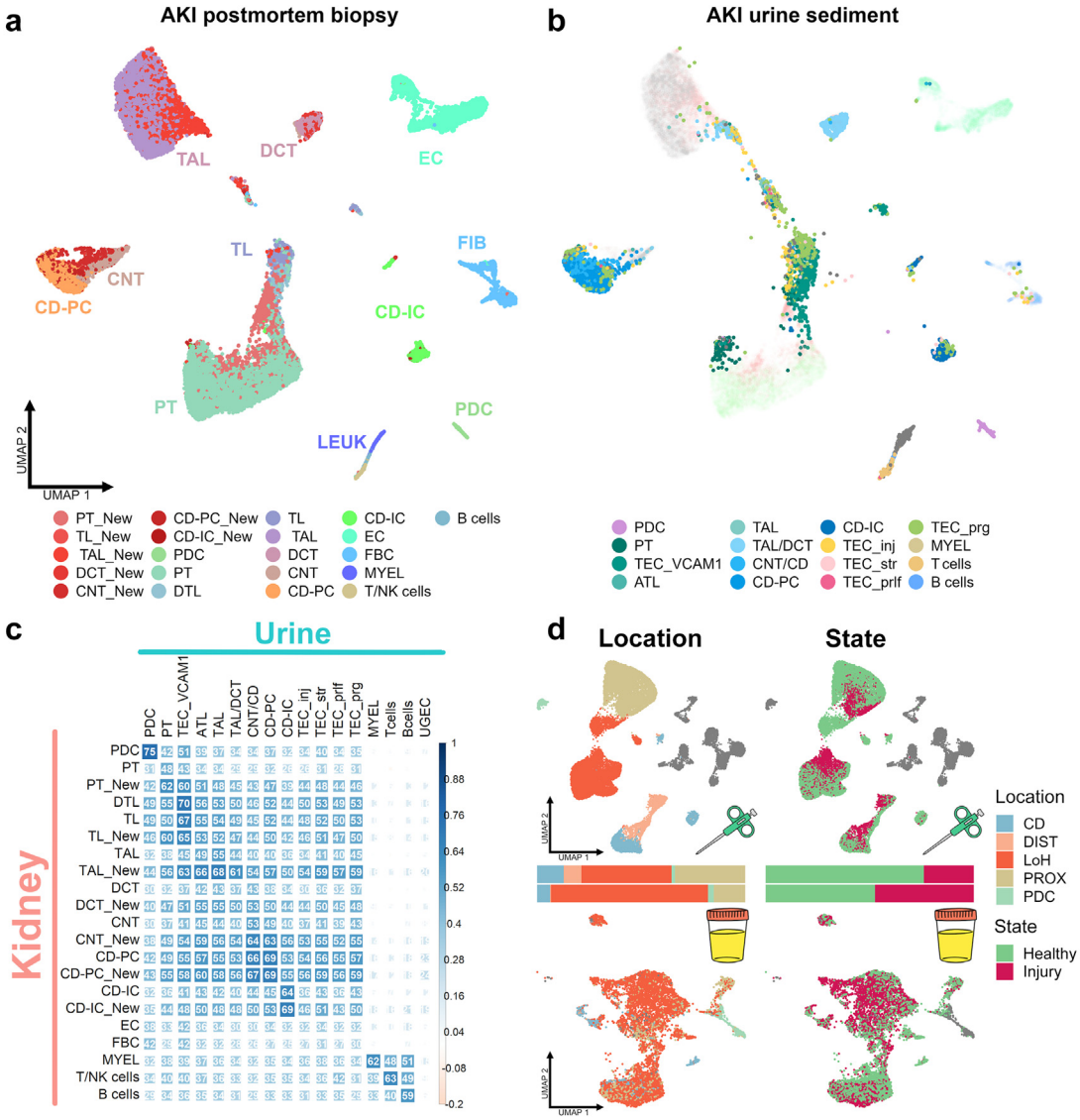

Figure 3 | Urinary cells from patients with acute kidney injury (AKI) mirror AKI postmortem biopsies. (**a**) Reference atlas of AKI postmortem biopsy single-nuclei RNA sequencing data.[12] (**b**) AKI urinary scRNAseq data mapped onto the tissue reference. Note how urine tubular epithelial cells (TECs) mostly overlap with kidney tissue injury-related cell types ("_New"; red shadings in **a**) and how few segment-specific urine TECs (green and blue shadings in **b**) cluster with respective tissue cell types. For alternative integration/comparison methods, see Supplementary Figures S9 and S10. (**c**) Correlation plot for gene expression of each 500 most variable expressed genes in urine (columns) and biopsy clusters (rows). Size and color represent the Spearman ρ (×100), all $P < 0.001$. Most urine TEC subsets correlate more closely with injured ("_New") tissue counterparts. (**d**) Uniform manifold approximation and projection (UMAP) distribution of epithelial single cells in biopsy (above) and urine (below) by location along the nephron (proximal [PROX], loop of Henle [LoH], distal [DIST], or collecting duct [CD]) and by state (healthy/injured). Note how urine excreted cells have a bias toward distal nephron segments and injured states. Endothelial and immune cells are in gray. Annotation of urine cells done by Symphony reference annotation. ATL, ascending thin limb; CD-IC, collecting duct intercalated cell; CD-PC, collecting duct principal cell; CNT, connecting tubule; DCT, distal convoluted tubule; DTL, descending thin limb; EC, endothelial cell; FIB, fibrocyte; inj, injury; LEUK, leukocyte; MYEL, myeloid cell; _New, AKI-reactive cell state; NK, natural killer; PDC, podocyte; prg, progenitor-like; prlf, proliferating; PT, proximal tubule; str, stressed; TAL, thick ascending limb; TL, loop of henle thin limb; VCAM1, vascular cell adhesion protein 1.

cell state of *progenitor-like cells* ("TEC_prg"; Figure 2e). The phenotype of these progenitor-like cells was further supported by automatic annotation using an expression atlas of human primary cells[28] as reference. Herein, most urinary renal cells were unsurprisingly annotated as epithelial cells, whereas a substantial fraction of TEC_prg was annotated as tissue or embryonic stem cells. (Supplementary Figure S8A and B). In addition, high expression of markers for kidney development[29,30] (*SOX4* and *CITED2*), stemness[31,32] (*PLCG2*, *HES1*, and *KLF4*), and differentiation processes[33–36] (*ELF3*, *IER2*, and *DDX17*) in these subsets (Supplementary Figure S8C) further underlines their regenerative potential.

The identity of one cluster, TEC_VCAM1, remained inconclusive, as it included cells with descending thin limb–

specific gene expression (*CPE*, *TNFSF10*, *AKR1B1*, and *AQP1*) but also showed high expression of *VCAM1* and *DCDC2* (Supplementary Figure S7), markers for the recently reported "failed-repair" adaptive cell state of the PT in AKI.[5]

All injury-related subsets weakly expressed PT markers (*GPX3*), thick ascending limb (TAL) markers (*SLC12A1/UMOD*), or collecting duct (CD) markers (*AQP2/FXYD4*), without coexpression of these markers in single cells (Supplementary Figure S8), indicating a preserved injury reaction from all nephron segments, which is not limited to the much-investigated PT.

Taken together, the phenotype of urinary TECs seemed to be primarily determined by injury-related dedifferentiation processes and only to a lesser extent by their tubule segment origin.

Urinary cells from patients with AKI mirror AKI postmortem biopsies

It is important to investigate to what extent urinary cells reflect kidney pathophysiology. Therefore, we used single-nuclei RNA sequencing data from human postmortem AKI kidney biopsies generated previously[12] (Figure 3a). Briefly, data of human AKI kidney tissue contained 106,971 single nuclei with transcriptomes indicating tubular, leukocyte, endothelial, and fibrocyte identities. In most nephron segments, Hinze *et al.* describe several injury-related altered tubular phenotypes, most notably inflammation, oxidative stress, and signs of epithelial-to-mesenchymal transition, herein annotated as PT_New, TL_New, TAL_New, DCT_New, CNT_New, CD-PC_New, and CD-IC_New.[12]

We used the biopsy AKI data to construct a reference atlas with symphony[37] and mapped our urine data onto the atlas (Figure 3a and b; a more conservative integration of data sets using harmony can be found in Supplementary Figure S9). This data overlap of urine and tissue validated our prior findings, with few urinary TECs mapping to healthy tissue TECs, most notably PT and CD. Injury-related urinary subsets mapped to injured biopsy cell states ("New_"), especially of TAL, thin limb (TL), and PT origin. The Map query also revealed low abundance of urinary fibrocytes and endothelial cells (Figure 3b) that had previously been clustered with TECs and leukocytes in the nonintegrated urine data (Figure 1).

Encouraged by these findings, we compared the gene expression between urine and biopsy data sets. Correlations of expression profiles showed molecular similarity of corresponding urine and tissue cell types (Figure 3c), and most urinary tubular subsets had a better expression correlation with injury-related "New" biopsy clusters than healthy counterparts.

Wanting to validate our findings with another approach, automated cell annotation (SingleR) of our urine data using AKI biopsy data as reference yielded similar results: Aside from small subsets of healthy, segment-specific tubular cells, urinary TECs appeared to be of injured phenotypes and derived mostly from loop of Henle and collecting duct segments of the tubule (Supplementary Figure S10).

Comparing nephron location and disease state (based on the reference atlas mapping) revealed a urinary bias toward medullary and distal injured nephron segments (Figure 3d). This indicates that the urinary renal cell signature is influenced by injured TECs being excreted following loss of tubular integrity and/or detachment from the basal membrane, with viable TAL, TL, and CD cells being more prone to final urinary excretion.

Further comparisons to public healthy kidney and bladder data sets supported the renal origin of these cells, whereas urine stress gene signatures suggested only a confined impact of urine exposure on the TEC transcriptome (for more detailed information, see Supplementary Results and Supplementary Figures S21 and S22). In conclusion, mostly injured and medullary TECs were excreted with urine, while information about tubular segment origin and pathophysiology was preserved in these cells.

Human urinary TECs resemble adaptive cell states of mouse AKI

We next determined whether our urinary TEC data reflect injury and adaptive cell states that have first been described in mouse AKI models. These states, including "injury," but also adaptive "repairing" and "failed-repair"[5,9] TECs, have since also been detected in human tissue samples.[8,12]

In a cross-species mouse/human comparative approach (see Methods), we trained a multinomial model using marker genes recently published in a mouse ischemia-reperfusion injury data set by Kirita *et al.*,[5] who initially described these adaptive cell states in the PT (Figure 4a and b). The model indicated that most urinary TEC clusters resembled "injured" cell states (Figure 4c). A portion of segment-specific clusters, mostly PT and TAL, were also assigned as "healthy." Interestingly, TEC_VCAM1 mostly resembled the "failed-repair" cell state, whereas TEC_prg overlapped with "repair" and "healthy" states (Figure 4c and d). These findings indicated a potential trajectory in the urine TECs from healthy to injured to adaptive cell states.

Urinary adaptive cell states are potentially derived from the thick ascending limb and show regenerative signatures

Urinary TECs mostly displayed dedifferentiated injury and adaptive phenotypes. To evaluate the origin of those cells, we investigated urine TEC data using monocle3, an algorithm for computational prediction of cell differentiation trajectories (Figure 5a and b). We observed a trajectory from a healthy TAL (*SLC12A1*$^+$, *UMOD*$^+$, *LCN2*$^-$) cluster through injured cell states (*LCN2*$^+$) to end points in presumably adaptive, dedifferentiated cell states TEC_prg (*SOX4*$^+$, *PAX2*$^+$) and TEC_VCAM1 (*VCAM1*$^+$, *PROM1*$^+$) (Figure 5c).

Interestingly, proximal TECs were not connected to this trajectory graph, potentially due to their comparatively low abundance in the urinary samples. Nevertheless, the PT cluster showed a separate, similar trajectory from differentiated (*LRP2*$^+$, *GPX3*$^+$) to injured/adaptive

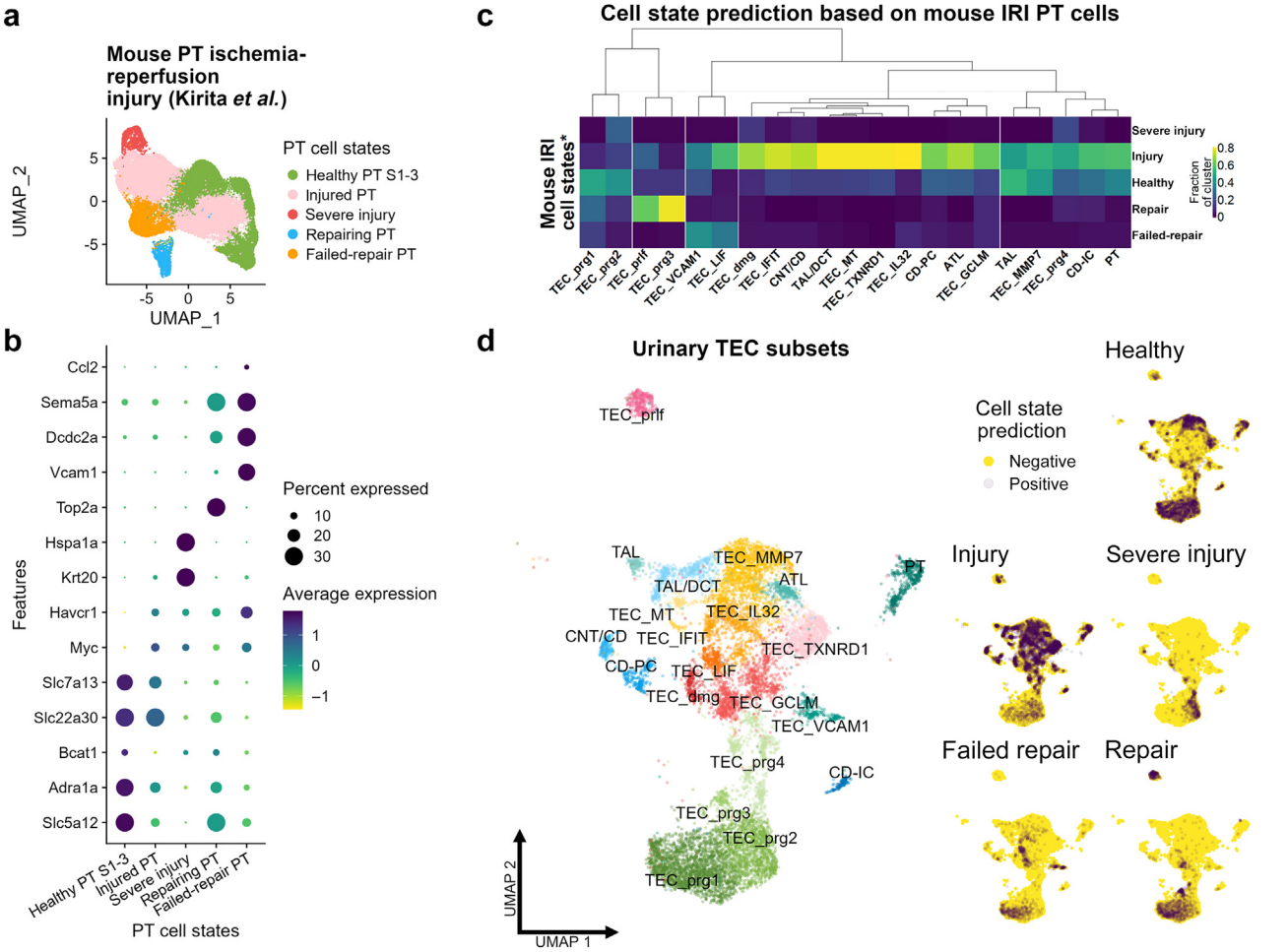

Figure 4 | Urinary tubular epithelial cells (TECs) resemble adaptive cell states of mouse acute kidney injury. (**a**) Uniform manifold approximation and projection (UMAP) and marker genes for proximal tubule (PT) dynamic cell states after ischemia-reperfusion injury (IRI) in a mouse model.[5] (**b**) Dot plot of relevant marker genes for clusters in (**a**). (**c**) Results from cross-species approach using data in (**a**) and (**b**) as reference. The color code indicates the percentage of urine TEC clusters that were assigned to the indicated mouse PT injury cell states. Most clusters are predominantly assigned to the injury cell state, whereas few other clusters (TEC_prg, TEC_prlf, TEC_LIF, and TEC_VCAM1) are assigned to adaptive cell states "repair" and "failed repair." (**d**) UMAP visualization. Dark shadings indicate assignment to the mouse PT injury cell state. Adaptive cell states can mainly be found in the bottom clusters. ATL, ascending thin limb; CD, collecting duct; CD-IC, collecting duct intercalated cell; CD-PC, collecting duct principal cell; CNT, connecting tubule; DCT, distal convoluted tubule; dmg, damage; GLCM, glutamate-cysteine ligase modifier subunit; IFIT, interferon induced protein with tetratricopeptide repeats; IL32, interleukin 32; LIF, leukemia inhibitory factor; MMP7, matrix metalloproteinase 7; MT, metallothioneins; prg, progenitor-like; prlf, proliferating; TAL, thick ascending limb; TXNRD1, thioredoxin reductase 1; VCAM1, vascular cell adhesion protein 1.

(*HAVCR1*$^+$, *VCAM1*$^+$, *PROM1*$^+$) states (Supplementary Figure S11).

This trajectory inference must be interpreted cautiously, as the starting point of the trajectory needs to be chosen by the investigator based on prior knowledge or assumption. However, several other observations suggest that the TEC_prg represents an injury adaptive cell state: Phospholipase C γ 2 (*PLCG2*), together with proliferation markers *FOS* and *JUN*, was among the most highly expressed genes in these clusters (Supplementary Figure S12). Although *PLCG2* is mostly associated with immune cells,[38] recent evidence for *PLCG2*-dependent signaling in epithelia[32,39] and in *in vitro* proliferation of hepatocytes[40] suggests a *role of PLCG2 in epithelial regeneration*, possibly via interactors in the fibroblast growth factor/extracellular signal-regulated kinase pathway[41] or Wnt pathways.[42] Fittingly, the AKI regeneration-associated pathways phosphatidylinositol-3′-kinase (PI3K),[43,44] estrogen,[45] and Wnt[42] (inferred by PROGENy) were more active in the TEC_prg clusters (Figure 5d). Also, embryogenesis/developmental transcription factors *PAX2*, *SOX4*, and *SOX9* were predominantly expressed in the presumed progenitor clusters, whereas other known surface stem cell markers, like *CD24*, *CD44*, and *PROM1*, were also expressed in the TEC_inj clusters (Supplementary Figure S12). Appropriately, gene signatures in *PAX2*$^+$ cells were similar to developmental terms found in the Gene Ontology database, many of them kidney specific, like "metanephric tubule development," with additional stem cell terms like "somatic stem cell population

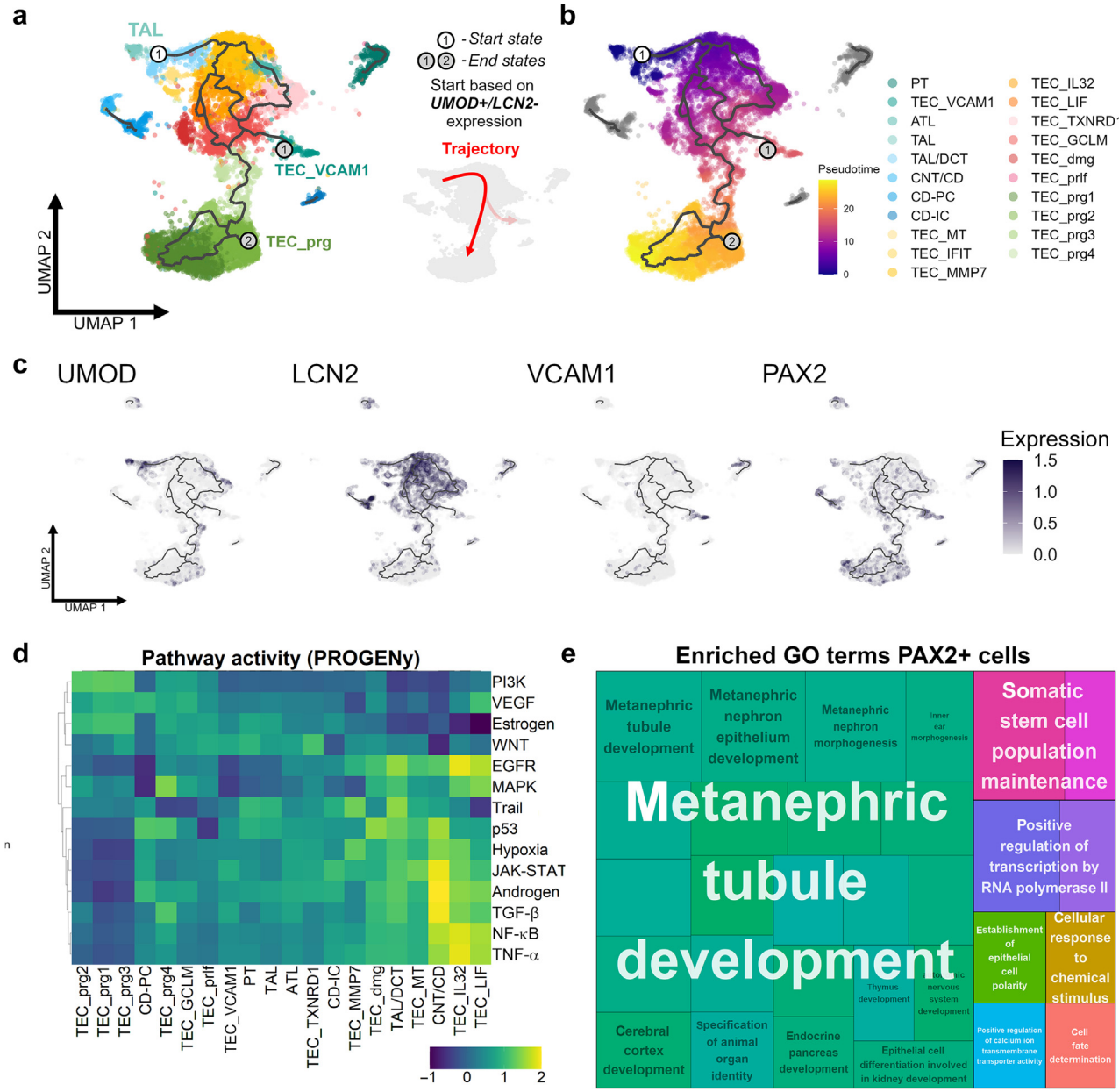

Figure 5 | Urinary adaptive cell states are potentially derived from the thick ascending limb (TAL) and show regenerative signatures. (**a,b**) Pseudotime trajectory analysis of urinary tubular epithelial cells (TECs) after acute kidney injury. A region with high TAL marker expression (uromodulin [*UMOD*]/solute carrier family 12 member 1 [*SLC12A1*]) and low injury marker expression (lipocalin 2 [*LCN2*]) was set as a starting state. Trajectory graph shows 2 end points in potentially adaptive cell states TEC_VCAM1 and TEC_prg. For separate trajectory analysis of proximal tubule (PT), see Supplementary Figure S11. (**c**) Expression of relevant marker genes across the trajectory (UMOD, TAL marker; LCN2, injury marker; vascular cell adhesion protein 1 [VCAM1], marker for "failed-repair" state in TECs; and paired box gene 2 [PAX2], kidney development marker). (**d**) Heat map of differing pathway activity in TEC clusters (inferred from PROGENy). Note the divide between progenitor-like (TEC_prg) and other subsets concerning regeneration-associated pathways (Wnt, phosphatidylinositol-3′-kinase [PI3K], and estrogen). (**e**) Treemap plot of enriched Gene Ontology (GO) terms in PAX2^{+} cells. Each rectangle is a single GO term (black text), sized based on –log10 (adjusted *P* value). The terms are joined into GO clusters by similarity, with the largest rectangle of the cluster providing the group name (white text). Data are visualized with different colors. ATL, ascending thin limb; CD, collecting duct; CD-IC, collecting duct intercalated cell; CD-PC, collecting duct principal cell; CNT, connecting tubule; DCT, distal convoluted tubule; dmg, damage; EGFR, epidermal growth factor receptor; GCLM, glutamate-cysteine ligase modifier subunit; IFIT, interferon induced protein with tetratricopeptide repeats; IL32, interleukin 32; JAK, janus kinases; LIF, leukemia inhibitory factor; MAPK, mitogen-activated protein kinase; MMP7, matrix metalloproteinase 7; MT, metallothioneins; NF-κB, nuclear factor-κB; prg, progenitor-like; prlf, proliferating; STAT, signal transducer and activator of transcription proteins; TGF-β, transforming growth factor-β; TNF-α, tumor necrosis factor-α; TXNRD1, thioredoxin reductase 1; VEGF, vascular endothelial growth factor.

maintenance," indicating a *developmental stage* (Figure 5e). Distinct cellular crosstalk of TEC_prg with epithelial and immune cells in comparison to other TECs further emphasized these findings (for more detailed information, see Supplementary Results and Supplementary Figure S23). *SOX4* and *SOX9* expression also increased in TAL and CD cells in biopsies obtained after AKI, indicating a similarity of the injury reaction between tissue and urine cells (Supplementary Figure S13).

In conclusion, these analyses suggest that TEC_prg may represent an adaptive cell state of potential TAL origin.

Urinary TEC abundance suggests temporal shift after AKI

One of the major advantages of cellular urinalysis is its repeatability, allowing to evaluate temporal changes after AKI onset more easily than biopsy-based approaches. Although our data set includes only a limited amount of repeatedly sampled patients and sampling time points varied, we nevertheless tried to extrapolate temporal changes in the urine sediment composition after AKI. We compared absolute TEC counts in different phases (Figure 6) after onset of AKI (early, up to 5 days after AKI onset; mid, day 6–10; and late, after day 10). Overall, the highest urinary TEC excretion seemed to happen from day 6 onward, with total TEC counts being significantly increased in patients sampled between days 6 and 10 ($P < 0.018$, unpaired 2-sample Wilcoxon test). This higher TEC count seems to be driven mainly by urinary shedding of TEC_inj and TEC_str after AKI, which both are significantly increased in the mid phase compared with early and late AKI ($P < 0.005$ and $P < 0.0059$, respectively). On the contrary, amounts of excreted TEC_prg remained unchanged in the analyzed time frame. The 6 repeatedly sampled patients (Figure 6c and Supplementary Figure S14) all hint at temporal shifts in the urine cell signature after AKI, but due to high interindividual variability in the AKI disease course, no definite conclusions on time-dependent changes can be drawn from the current data set.

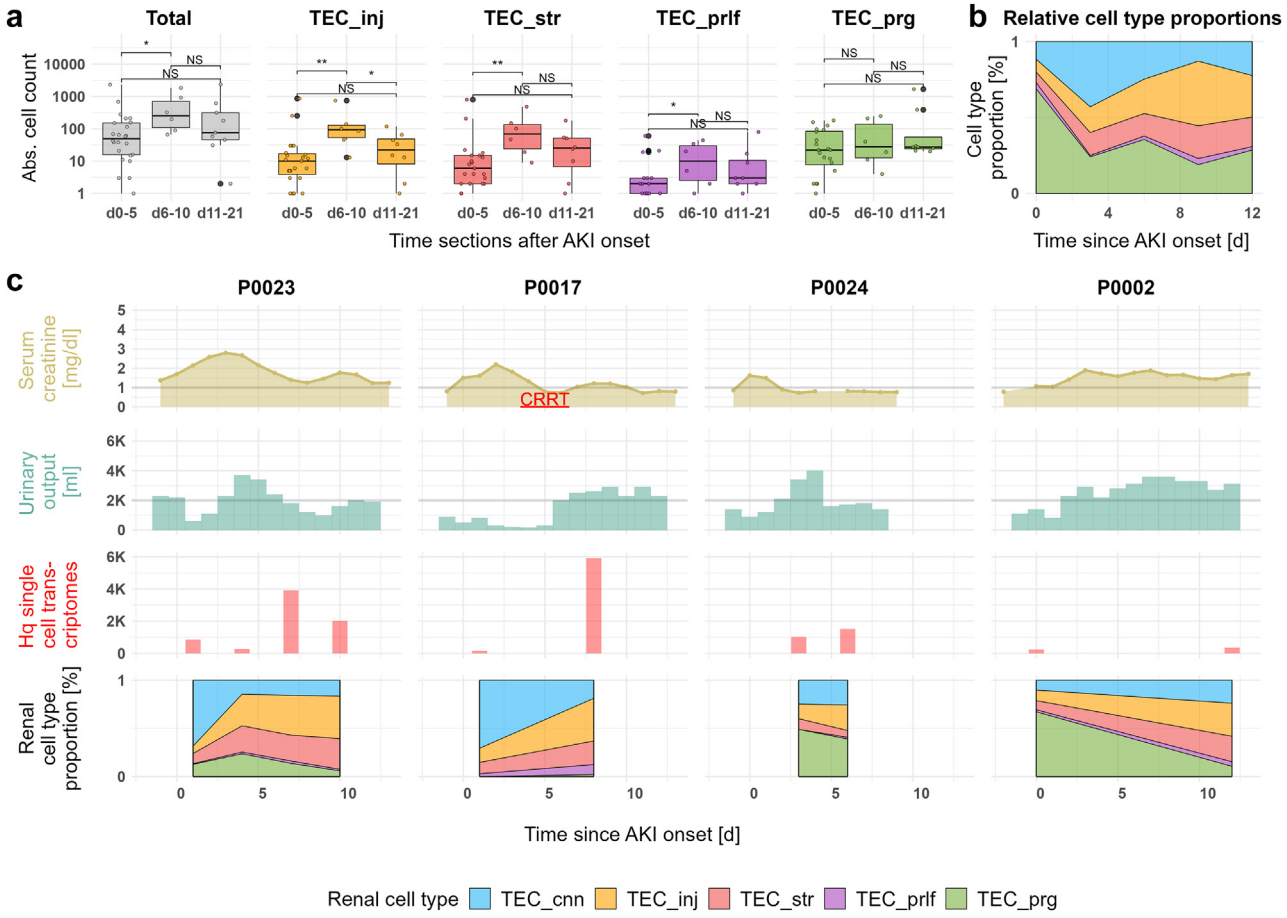

Figure 6 | Urinary acute kidney injury (AKI) tubular epithelial (TEC) cell abundance and cell type proportions at different time points. (**a**) Absolute amount of urinary renal TECs and subsets by patient at different time points. Excretion of TEC peaks around day (d) 5 to 10, mainly via more injured cell types (TEC_inj and TEC_str). (**b**) Relative TEC subset proportions at different time points. (Samples were binned by time point in 3-day intervals. The mean proportion of cell type across samples in each bin was calculated.) (**c**) Individual AKI course over time with serum creatinine, urinary output, single-cell transcriptome yield, and relative amount of urinary renal parenchymal cell subsets; compare also Supplementary Figure S14. Box plot: line = median, hinges = first-third quartile, whiskers = 1.5 interquartile range, and large dots = outliers. *$P < 0.05$, **$P < 0.01$, ***$P < 0.001$, and ****$P < 0.0001$, unpaired 2-sample Wilcoxon test. cnn, canonical; inj, injury; NS, not significant; prg, progenitor-like; prlf, proliferating; str, oxidative stress.

DISCUSSION

This study positions urinary scRNAseq as a new, powerful tool to study human AKI. Kidney parenchymal cells, including TECs and podocytes, can reliably be detected in urine of patients with AKI. These urine-excreted kidney cells mirror findings in transcriptional analyses of human and mouse AKI tissue.

Feasibility of urinary scRNAseq

Urinary scRNAseq has now been tested in several credible cohorts[18,19,46] across different diseases. These studies revealed a high variability of the viable cell count across samples. This variability likely relates to disease severity but is probably also influenced by varying sample sizes due to fluctuating urinary output (Supplementary Figure S2B). Two strategies to overcome this issue are (i) pooling of multiple samples and (ii) repeated sampling of the same patient over time, both of which were successfully applied herein.

The urinary cellular signal, independent from disease type or severity, is dominated by leukocytes and urogenital epithelia.[18,19] Therefore, most urinary cellular studies, single cell[47] or otherwise,[14,16,48] have focused on analyses of urinary immune cells. Herein, we demonstrate that by flow cytometric preselection and gathering of sufficient viable cell counts, the focus of urinary cellular analysis can be shifted toward renal parenchymal cells.

Urogenital cells were more frequent in female patients (Supplementary Figure S5). This could theoretically be attributed to anatomic differences of the lower urinary tract in female patients compared with male patients. However, most urine samples for this study were gained through bladder catheters. It appears therefore that bladder cells are more easily and more frequently shedded in female patients. However, this assumption certainly requires further investigation. The high variability of urogenital epithelial cell abundance between men and women and between cohorts (Supplementary Figure S18) also suggests that standardized sampling methods will be crucial for the comparison of urine signatures, as factors like sample preparation (e.g., flow sort of viable cells) seem to influence urine sediment composition.

Comparison with human AKI tissue data

Urinary TEC transcriptomes correlate well with respective reference cells from tissue and mirror the damaged and injured TEC phenotypes in postmortem AKI biopsy samples. This result is essential as it shows that the molecular makeup of TEC is sufficiently preserved in urine to infer data informative about molecular expression patterns in a patient's kidney without biopsies. Moreover, together with the data by Hinze *et al.*,[12] our results challenge the proximal tubular centricity of (murine) AKI research, with other nephron segments, especially TAL, seemingly contributing to injury-related cell pools as much as PT cells.[11] Urine appears to be especially suited to study changes in the more distal nephron segments, as those TECs seem to be preferentially excreted into urine.

Injury-related tubular cell states in the urine

Our current understanding of TEC injury reaction assumes an adaptive repair process involving dedifferentiation and redifferentiation, which has been demonstrated for PT cells in several mouse models,[5,8,9] and cells in human AKI biopsies have been reported to mirror this process.[8,11,12]

In our urine AKI data, most TECs (TEC_inj and TEC_str) seem to be of an early injured phenotype, as referencing with human tissue data (Figure 3) and comparison with mouse ischemia-reperfusion injury cell states (Figure 4) suggest. However, the lack of segment-specific marker genes as well as inflammatory and epithelial-to-mesenchymal transition signatures suggests a beginning dedifferentiation/adaptation process even in these cells.

Other TEC subsets (TEC_prg, TEC_VCAM1, and TEC_prlf) are more likely to mirror the adaptive repair process in the urine: Pseudotime analysis suggests TEC_prg may represent an adaptive cell state of TAL origin (Figure 5a and b), which was recently described in human AKI tissue alongside the much better characterized PT adaptive states.[11] Fittingly, TEC_prg mapped mostly to TAL and TL cells in the AKI reference atlas (Figure 3b). In the cross-species approach, TEC_prg was assigned as "repair" or "healthy" state, further emphasizing a regenerative potential. Similar $SOX4^{+}SOX9^{+}$ cells occur in the reference kidney biopsy tissue samples after AKI (Supplementary Figure S13). Other diseases, like diabetic nephropathy and focal segmental glomerular sclerosis, seemed to have a lower abundance of TEC_prg in the urine compared with AKI (Supplementary Results and Supplementary Figure S20), whereas the occurrence of similar progenitor-like cells in the urine is not entirely unprecedented.[21,49]

Another cluster in the urine TEC data highly expressed *VCAM1* (TEC_VCAM1), a marker recently associated with the maladaptive "failed-repair" state in the PT. Cross-species comparison also suggested that this cluster is the most likely to represent the "failed-repair" state (Figure 4c and d), whereas pseudotime analysis showed TEC_VCAM1 as a trajectory end point alongside TEC_prg (Figure 5a and b). However, these results must be interpreted cautiously: The trajectory graph does not link to the healthy PT subset, which is the known origin for "failed-repair" cells. Instead, the limited number of PT cells in urine showed a similar but distinct dedifferentiation trajectory (Supplementary Figure S11). The TEC_VCAM1 cluster also expressed several markers hinting at a descending thin limb segment–specific lineage. So, whether TEC_VCAM1 is a urine equivalent of the injury adaptive "failed-repair" state cannot be fully clarified with the current data set.

Study limitations

Although urinary scRNAseq enables safe and easily repeatable examination of kidney cells in AKI, it is limited to patients

with preserved diuresis, therefore excluding a substantial part of severe, oligo-to-anuric AKI cases from analysis. Because healthy donors usually excrete almost no TECs, urinary data cannot be compared with a healthy urinary control group (see also Supplementary Results). Although our findings are overlapping well with reference tissue data, the extent to which urinary analysis reflects the individual disease course remains uncertain, as gathering of urine and concurrent biopsy tissue from the same patient was not possible.

Our method currently requires immediate processing of fresh urine samples, thus limiting its use for prospective clinical and research applications. This implies that a repeated sampling at preplanned dates was frequently not possible, limiting the meaningfulness of our data concerning time course and outcome analysis.

Conclusions

With the present data set, we demonstrate feasibility of urinary scRNAseq in human AKI. The epithelial cells detected in the urine originate mainly from the distal nephron segments and reflect changes observed in murine and human kidney tissue. With further standardization of sample collection and conservation, noninvasive and temporally resolved pathophysiological insights through urinary scRNAseq may facilitate kidney diagnostics and monitoring.

DISCLOSURE

All the authors declared no competing interests.

DATA STATEMENT

Sequencing data have been deposited in Gene Expression Omnibus under accession code GSE199321. Code is available under https://github.com/janklocke/Urine-single-cell-sequencing-AKI.

ACKNOWLEDGMENTS

This work was supported by grants from the Berlin Institute of Health, the Jackstädt-Stiftung, the Deutsche Forschungsgemeinschaft (DFG; HI 2238/2-1), and Bundesministerium für Bildung und Forschung. JK was supported by a research scholarship of the Deutsche Gesellschaft für Nephrologie. KMS-O was supported by the DFG (SFB 1365, GRK 2318, and FOR 2841). We thank the Flow Cytometry and Cell Sorting Facility and laboratory managers at Deutsches Rheuma-orschungszentrum Berlin for technical support and helpful insights. We thank all staff at the Charité's nephrology, cardiac surgery, and intensive care wards for helping with sample collection; and we thank all patients for participating.

AUTHOR CONTRIBUTIONS

JK, K-UE, CK, NR, and PE designed the study. JK, CMS, AB, DM, EG, LP, LW, PF, NG, FM, M-FM, and PE conducted experiments and acquired data. JK, SJK, CMS, CH, CK, and PE analyzed data. JK, SJK, CMS, CH, KMS-O, M-FM, CK, K-UE, NR, and PE interpreted the results. JK, CK, K-UE, and PE wrote the manuscript.

SUPPLEMENTARY MATERIAL

Supplementary File (PDF)

Figure S1. Study design and patient characteristics.

Figure S2. Flow cytometry can provide viable presorted urine cell fractions.

Figure S3. Urine single-cell libraries can be demultiplexed after hashing and pooling of samples.

Figure S4. Amount of captured urinary is diverse.

Figure S5. Urogenital cell abundance in urine is higher in female patients.

Figure S6. Diverse tubular cell reactions to acute kidney injury (AKI).

Figure S7. Injured cell states are of mixed tubular identity.

Figure S8. Urinary tubular epithelial cells partially resemble stem cells.

Figure S9. Urinary cells from patients with acute kidney injury (AKI) mirror AKI postmortem biopsies.

Figure S10. Urinary tubular cells resemble injured and distal tubules.

Figure S11. Urinary proximal tubular epithelial cell dedifferentiation trajectory.

Figure S12. Urinary tubular epithelial cells show regenerative phenotypes.

Figure S13. $SOX4^{+}SOX9^{+}$ progenitor-like cells occur in kidney acute kidney injury (AKI) tissue.

Figure S14. Urinary acute kidney injury (AKI) tubular epithelial cell abundance and cell type proportions at different time points.

Supplementary Methods.

Supplementary Results.

Figure S15. Healthy urine sediment is almost devoid of kidney and immune cells.

Figure S16. Tubular epithelial cell abundance is dependent on acute kidney injury (AKI) etiology.

Figure S17. Urine cells show coronavirus disease 2019 (COVID-19)–associated transcriptional signatures.

Figure S18. Disease type influences urine cellular abundance and composition.

Figure S19. Adaptive progenitor-like cell abundance is increased in acute kidney injury (AKI).

Figure S20. Adaptive progenitor-like cell abundance is increased in acute kidney injury (AKI).

Figure S21. Urine tubular cells cluster with kidney, not bladder, tissue.

Figure S22. Stress genes are partially upregulated in urine cells.

Figure S23. Subset-specific cellular crosstalk of urinary tubular cells.

Supplementary References.

Supplementary File (Excel)

Table S1. Patient characteristics.

Supplementary File (Excel)

Table S2. Differentially expressed genes for clusters of all urine cells.

Supplementary File (Excel)

Table S3. Differentially expressed genes for clusters of all kidney parenchymal cells.

REFERENCES

1. Lafrance JP, Miller DR. Acute kidney injury associates with increased long-term mortality. *J Am Soc Nephrol*. 2010;21:345–352.
2. Sawhney S, Marks A, Fluck N, et al. Intermediate and long-term outcomes of survivors of acute kidney injury episodes: a large population-based cohort study. *Am J Kidney Dis*. 2017;69:18–28.
3. Qi R, Yang C. Renal tubular epithelial cells: the neglected mediator of tubulointerstitial fibrosis after injury. *Cell Death Dis*. 2018;9:1–11.
4. Liu BC, Tang TT, Lv LL. How tubular epithelial cell injury contributes to renal fibrosis. *Adv Exp Med Biol*. 2019;1165:233–252.
5. Kirita Y, Wu H, Uchimura K, et al. Cell profiling of mouse acute kidney injury reveals conserved cellular responses to injury. *Proc Natl Acad Sci U S A*. 2020;117:15874–15883.
6. Rudman-Melnick V, Adam M, Potter A, et al. Single-cell profiling of AKI in a murine model reveals novel transcriptional signatures, profibrotic

phenotype, and epithelial-to-stromal crosstalk. *J Am Soc Nephrol*. 2020;31:2793–2814.
7. Little M, Humphreys B. Regrow or repair: an update on potential regenerative therapies for the kidney. *J Am Soc Nephrol*. 2022;33:15–32.
8. Legouis D, Rinaldi A, Arnoux G, et al. Single cell profiling in COVID-19 associated acute kidney injury reveals patterns of tubule injury and repair in human. Preprint. *bioRxiv*. 463150. Posted online October 6, 2021. https://doi.org/10.1101/2021.10.05.463150
9. Ide S, Kobayashi Y, Ide K, et al. Ferroptotic stress promotes the accumulation of pro-inflammatory proximal tubular cells in maladaptive renal repair. *eLife*. 2021;10:e68603.
10. Chang-Panesso M, Kadyrov FF, Lalli M, et al. FOXM1 drives proximal tubule proliferation during repair from acute ischemic kidney injury. *J Clin Invest*. 2019;129:5501–5517.
11. Lake BB, Menon R, Winfree S, et al. An atlas of healthy and injured cell states and niches in the human kidney. Preprint. *bioRxiv*. 454201. Published online July 29, 2021. https://doi.org/10.1101/2021.07.28.454201
12. Hinze C, Kocks C, Leiz J, et al. Single-cell transcriptomics reveals common epithelial response patterns in human acute kidney injury. *Genome Med*. 2022;14:103.
13. Goerlich N, Brand HA, Langhans V, et al. Kidney transplant monitoring by urinary flow cytometry: biomarker combination of T cells, renal tubular epithelial cells, and podocalyxin-positive cells detects rejection. *Sci Rep*. 2020;10:796.
14. Klocke J, Kopetschke K, Grießbach AS, et al. Mapping urinary chemokines in human lupus nephritis: potentially redundant pathways recruit CD4+ and CD8+ T cells and macrophages. *Eur J Immunol*. 2017;47:180–192.
15. Bertolo M, Baumgart S, Durek P, et al. Deep phenotyping of urinary leukocytes by mass cytometry reveals a leukocyte signature for early and non-invasive prediction of response to treatment in active lupus nephritis. *Front Immunol*. 2020;11:256.
16. Dolff S, Abdulahad WH, Arends S, et al. Urinary CD8+ T-cell counts discriminate between active and inactive lupus nephritis. *Arthritis Res Ther*. 2013;15:R36.
17. Kujat J, Langhans V, Brand H, et al. Monitoring tubular epithelial cell damage in AKI via urine flow cytometry. Preprint. *medRxiv*. 22270101. Posted online February 1, 2022. https://doi.org/10.1101/2022.01.31.22270101
18. Abedini A, Zhu YO, Chatterjee S, et al. Urinary single-cell profiling captures the cellular diversity of the kidney. *J Am Soc Nephrol*. 2021;32:614–627.
19. Latt KZ, Heymann J, Jessee JH, et al. Urine single cell RNA-sequencing in focal segmental glomerulosclerosis reveals inflammatory signatures. *Kidney Int Rep*. 2021;7:289–304.
20. Wang Y, Zhao Y, Zhao Z, et al. Single-cell RNA-seq analysis identified kidney progenitor cells from human urine. *Protein Cell*. 2021;12:305–312.
21. Lazzeri E, Ronconi E, Angelotti ML, et al. Human urine-derived renal progenitors for personalized modeling of genetic kidney disorders. *J Am Soc Nephrol*. 2015;26:1961–1974.
22. Rahman MS, Wruck W, Spitzhorn LS, et al. A comprehensive molecular portrait of human urine-derived renal progenitor cells. Preprint. Posted online April 8, 2019. *bioRxiv*. 602417.
23. Bento G, Shafigullina AK, Rizvanov AA, et al. Urine-derived stem cells: applications in regenerative and predictive medicine. *Cells*. 2020;9:573.
24. R: The R project for statistical computing. Accessed February 12, 2022. https://www.r-project.org/
25. Clatworthy MR. How to find a resident kidney macrophage: the single-cell sequencing solution. *J Am Soc Nephrol*. 2019;30:715–716.
26. Morse C, Tabib T, Sembrat J, et al. Proliferating SPP1/MERTK-expressing macrophages in idiopathic pulmonary fibrosis. *Eur Respir J*. 2019;54:1802441.
27. Montford JR, Bauer C, Dobrinskikh E, et al. Inhibition of 5-lipoxygenase decreases renal fibrosis and progression of chronic kidney disease. *Am J Physiol Renal Physiol*. 2019;316:F732–F742.
28. Mabbott NA, Baillie JK, Brown H, et al. An expression atlas of human primary cells: inference of gene function from coexpression networks. *BMC Genomics*. 2013;14:632.
29. Huang J, Arsenault M, Kann M, et al. The transcription factor Sry-related HMG box-4 (SOX4) is required for normal renal development *in vivo*. *Dev Dyn*. 2013;242:790–799.
30. Boyle S, Shioda T, Perantoni AO, de Caestecker M. Cited1 and Cited2 are differentially expressed in the developing kidney but are not required for nephrogenesis. *Dev Dyn*. 2007;236:2321–2330.
31. Liu ZH, Dai XM, Du B. Hes1: a key role in stemness, metastasis and multidrug resistance. *Cancer Biol Ther*. 2015;16:353–359.
32. Chan JM, , Quintanal-Villalonga Á, Gao VR, et al. Signatures of plasticity, metastasis, and immunosuppression in an atlas of human small cell lung cancer. *Cancer Cell*. 2021;39:1479–1496.e18.
33. Ng AYN, Waring P, Ristevski S, et al. Inactivation of the transcription factor Elf3 in mice results in dysmorphogenesis and altered differentiation of intestinal epithelium. *Gastroenterology*. 2002;122:1455–1466.
34. Oliver JR, Kushwah R, Wu J, et al. Elf3 plays a role in regulating bronchiolar epithelial repair kinetics following Clara cell-specific injury. *Lab Invest*. 2011;91:1514–1529.
35. Suthapot P, Xiao T, Felsenfeld G, et al. The RNA helicases DDX5 and DDX17 facilitate neural differentiation of human pluripotent stem cells NTERA2. *Life Sci*. 2022;291:120298.
36. Wu W, Zhang X, Lv H, et al. Identification of immediate early response protein 2 as a regulator of angiogenesis through the modulation of endothelial cell motility and adhesion. *Int J Mol Med*. 2015;36:1104–1110.
37. Kang JB, Nathan A, Weinand K, et al. Efficient and precise single-cell reference atlas mapping with Symphony. *Nat Commun*. 2021;12:5890.
38. Lampson BL, Brown JR. Are BTK and PLCG2 mutations necessary and sufficient for ibrutinib resistance in chronic lymphocytic leukemia? *Expert Rev Hematol*. 2018;11:185–194.
39. Elmentaite R, Kumasaka N, Roberts K, et al. Cells of the human intestinal tract mapped across space and time. *Nature*. 2021;597:250–255.
40. Ma D, Lian F, Wang X. PLCG2 promotes hepatocyte proliferation *in vitro* via NF-κB and ERK pathway by targeting bcl2, myc and ccnd1. *Artif Cells Nanomed Biotechnol*. 2019;47:3786–3792.
41. Xu Z, Zhu X, Wang M, et al. FGF/FGFR2 protects against tubular cell death and acute kidney injury involving Erk1/2 signaling activation. *Kidney Dis*. 2020;6:181–194.
42. Brossa A, Papadimitriou E, Collino F, et al. Role of CD133 molecule in Wnt response and renal repair. *Stem Cells Transl Med*. 2018;7:283–294.
43. Meng F, Zhang Z, Chen C, et al. PI3K/AKT activation attenuates acute kidney injury following liver transplantation by inducing FoxO3a nuclear export and deacetylation. *Life Sci*. 2021;272:119119.
44. Zhang G, Wang Q, Wang W, et al. Tempol protects against acute renal injury by regulating PI3K/Akt/mTOR and GSK3β signaling cascades and afferent arteriolar activity. *Kidney Blood Press Res*. 2018;43:904–913.
45. Buléon M, Cuny M, Grellier J, et al. A single dose of estrogen during hemorrhagic shock protects against kidney injury whereas estrogen restoration in ovariectomized mice is ineffective. *Sci Rep*. 2020;10:17240.
46. Cheung MD, Erman EN, Liu S, et al. Single-cell RNA sequencing of urinary cells reveals distinct cellular diversity in COVID-19-associated AKI. *Kidney360*. 2022;3:28–36.
47. Arazi A, Rao DA, Berthier CC, et al. The immune cell landscape in kidneys of patients with lupus nephritis. *Nat Immunol*. 2019;20:902–914.
48. Kopetschke K, Klocke J, Grießbach AS, et al. The cellular signature of urinary immune cells in lupus nephritis: new insights into potential biomarkers. *Arthritis Res Ther*. 2015;17:94.
49. Oliveira Arcolino F, Tort Piella A, Papadimitriou E, et al. Human urine as a noninvasive source of kidney cells. *Stem Cells Int*. 2015;2015:362562.